

Outdoor Synthetic Aperture Acoustic Ground Target Measurements

Steven Bishop^a, Therese-Ann Ngaya^b, Joe Vignola^b, John Judge^b,
Jay Marble^a, Pete Gugino^a, Mehrdad Soumekh^c, Erik Rosen^d

^aUS Army RDECOM CERDEC NVESD 10221 Burbeck Rd., Ft. Belvoir, VA 22060

^bThe Catholic University of America, 620 Michigan Ave. Washington, D.C. 20054

^cMehrdad Soumekh, Soumekh Consultant, Bethesda, MD, 20817

^dErik Rosen, IDA, 4850 Mark Center Drive, Alexandria, VA 22311

ABSTRACT

A novel outdoor synthetic aperture acoustic (SAA) system consists of a microphone and loudspeaker traveling along a 6.3-meter rail system. This is an extension from a prior indoor laboratory measurement system in which selected targets were insonified while suspended in air. Here, the loudspeaker and microphone are aimed perpendicular to their direction of travel along the rail. The area next to the rail is insonified and the microphone records the reflected acoustic signal, while the travel of the transceiver along the rail creates a synthetic aperture allowing imaging of the scene. Ground surfaces consisted of weathered asphalt and short grass. Several surface-laid objects were arranged on the ground for SAA imaging. These included rocks, concrete masonry blocks, grout covered foam blocks; foliage obscured objects and several spherical canonical targets such as a bowling ball, and plastic and metal spheres. The measured data are processed and ground targets are further analyzed for characteristics and features amenable for discrimination. This paper includes a description of the measurement system, target descriptions, synthetic aperture processing approach and preliminary findings with respect to ground surface and target characteristics.

Keywords: Synthetic aperture acoustics, side attack munitions, acoustic image, image reconstructions

1. INTRODUCTION

This paper describes a synthetic aperture acoustic (SAA) measurement system that is being studied for its ability to quantitatively report on the ground surface characteristics and characteristics of surface-laid targets, e.g., false targets such as natural rocks, foliage obscured side attack landmines and 155 mm munitions. The system supports a desired standoff detection capability by looking perpendicular to the direction of travel. The sensor's field of view is different from forward-looking radar⁽¹⁻⁵⁾ or other opto-acoustic systems,⁽⁶⁻⁸⁾ but addresses the lateral view of the standoff detection objective. Opto-acoustic and other excitation systems have been used successfully to detect buried landmines.⁽⁹⁻¹⁶⁾ Here, we constructed an acoustic transceiver (quasi-monostatic) mounted on a 6.3-meter portable rail system to facilitate controlled outdoor measurements (ultimately, the objective is a teleoperated vehicular mounted version). The direct measurement of the transceiver is the acoustic reflectivity found in the synthetic aperture or "acoustic scene". The acoustic absorption of some materials is frequency dependent⁽¹⁷⁾, and the frequency spectrum of the backscatter is also strongly influenced by the target geometry when the target dimensions are comparable to or greater than the acoustic wavelength⁽¹⁸⁾. In experiments described below, we imaged a number of targets and observed variations in acoustic reflectivity and phase versus aspect angle. Advanced signal processing systems for target discrimination based on shape, size and material may be found in the literature,⁽¹⁹⁻²²⁾ and will be considered in future research. In Section 2 we discuss the basic design of the of the measurement system. The targets are described in Section 3, and in Section 4 we briefly discuss the image processing technique, but dwell more on the characteristics and features of the ground surface and selected targets. In Section 5 we summarize the paper.

2. CHARACTERISTICS OF THE MEASUREMENT SYSTEM

In this application, SAA serves as a noninvasive inspection technology offering a standoff distance that provides a measure of safety for military personnel and equipment. Table 1 below contains system parameters of the current

REPORT DOCUMENTATION PAGE					<i>Form Approved OMB No. 0704-0188</i>	
The public reporting burden for this collection of information is estimated to average 1 hour per response, including the time for reviewing instructions, searching existing data sources, gathering and maintaining the data needed, and completing and reviewing the collection of information. Send comments regarding this burden estimate or any other aspect of this collection of information, including suggestions for reducing the burden, to Department of Defense, Washington Headquarters Services, Directorate for Information Operations and Reports (0704-0188), 1215 Jefferson Davis Highway, Suite 1204, Arlington, VA 22202-4302. Respondents should be aware that notwithstanding any other provision of law, no person shall be subject to any penalty for failing to comply with a collection of information if it does not display a currently valid OMB control number.						
PLEASE DO NOT RETURN YOUR FORM TO THE ABOVE ADDRESS.						
1. REPORT DATE (DD-MM-YYYY) April 19, 2010		2. REPORT TYPE Technical		3. DATES COVERED (From - To) 1 Jan 2009 - 31 Dec 2009		
4. TITLE AND SUBTITLE Outdoor Synthetic Aperture Acoustic Ground Target Measurements				5a. CONTRACT NUMBER NA		
				5b. GRANT NUMBER W911NF-07-R-0003-02		
				5c. PROGRAM ELEMENT NUMBER 0603606A		
6. AUTHOR(S) Bishop, Steven; Ngaya, Therese-Ann; Vignola, Joseph; Judge, John; Marble, Jay; Gugino, Pete; Soumekh, Mehrdad; Rosen, Erik				5d. PROJECT NUMBER NA		
				5e. TASK NUMBER NA		
				5f. WORK UNIT NUMBER NA		
7. PERFORMING ORGANIZATION NAME(S) AND ADDRESS(ES) The Catholic University of America, 620 Michigan Ave. Washington, D.C. 20054				8. PERFORMING ORGANIZATION REPORT NUMBER NA		
9. SPONSORING/MONITORING AGENCY NAME(S) AND ADDRESS(ES) US Army RDECOM CERDEC NVESD 10221 Burbeck Rd., Ft. Belvoir, VA 22060				10. SPONSOR/MONITOR'S ACRONYM(S) RDER-NVC-GV		
				11. SPONSOR/MONITOR'S REPORT NUMBER(S) NA		
12. DISTRIBUTION/AVAILABILITY STATEMENT Approved for public release; distribution is unlimited.						
13. SUPPLEMENTARY NOTES NA						
14. ABSTRACT A novel outdoor synthetic aperture acoustic (SAA) system consists of a microphone and loudspeaker traveling along a 6.3-meter rail system. This is an extension from a prior indoor laboratory measurement system in which selected targets were insonified while suspended in air. Here, the loudspeaker and microphone are aimed perpendicular to their direction of travel along the rail. The area next to the rail is insonified and the microphone records the reflected acoustic signal, while the travel of the transceiver along the rail creates a synthetic aperture allowing imaging of the scene. Ground surfaces consisted of weathered asphalt and short grass. Several surface-laid objects were arranged on the ground for SAA imaging. These included rocks, concrete masonry blocks, grout covered foam blocks; foliage obscured objects and several spherical canonical targets such as a bowling ball, and plastic and metal spheres. The measured data are processed and ground targets are further analyzed for characteristics and features amenable for discrimination. This report includes a description of the measurement system, target designations, synthetic aperture processing approach and						
15. SUBJECT TERMS Synthetic aperture acoustics, side attack munitions, acoustic image, image reconstructions						
16. SECURITY CLASSIFICATION OF:			17. LIMITATION OF ABSTRACT SAR	18. NUMBER OF PAGES 10	19a. NAME OF RESPONSIBLE PERSON Steven Bishop	
a. REPORT U	b. ABSTRACT U	c. THIS PAGE U			19b. TELEPHONE NUMBER (Include area code) (703) 704-1037	

outdoor SAA system. For these measurements a rail based system was constructed so that data could be collected during a continuous scan. Data presented here were collected while the acoustic transceiver was moving with a speed of 12 cm/s over the 5 m travel aperture. This is in contrast to previously reported indoor measurements,⁽²³⁾ where the system was manually moved 300 times in 1 cm increments over the travel range to gather a complete data set. A photograph of a typical outdoor setup is found in Figure 1 below. The rail is a fiberglass ladder support at intervals by adjustable legs to permit leveling and even load distribution. The tripod supporting the transceiver is fixed on a controlled motor driven platform. The system is capable of collecting data in both directions traveling along the rail. The acoustic source is a Pyramid[®] 1200 W TW67 speaker with a diaphragm approximately 12 cm in diameter. The microphone is a SBWA MPA 416 housed in the base of a common plastic funnel. The microphone is held in the center and base of the funnel by a foam grommet.

The excitation signals broadcast by the source were linear FM chirps that had been windowed. The frequency band of the excitation was 1-17 kHz and time duration was 10ms. These excitation signals were produced by a LabView[®] program, run on a PC, and routed through a power amplifier. Synchronous digitization of the received backscatter collected by the microphone was controlled by the same program. The PC and support electronics were housed in a mobile rack shown in Figure 2. Figure 2 also includes a photograph of a typical experimental setup where a number of targets were laid out within the measurement domain of the SAA system.

Table 1 Characteristics of the synthetic aperture acoustic system.

Parameter	Nomenclature	Estimated Value
Wave propagation speed	c	340 m/s
Carrier frequency	f_o	10 kHz
Carrier wavelength	$\lambda_o = c/f_o$	0.034 m
Chirp bandwidth	B_c	16 kHz
Chirp time length	T_c	10 msec
Range resolution	$\delta_{\text{range}} = c/(2B_c)$	0.011 m
Aperture length	D	0.12 m
Aperture beamwidth	$\theta_B \approx \lambda_o/D$	0.28 rad
Target range	x_o	[3-5.5] m
Along-track resolution	$\delta_{\text{along-track}} = D/2$	0.06 m
Pulse repetition frequency ¹	PRF	16.67 Hz
Vehicle speed	v	0.012 m/s

¹ The inter pulse period (IPP) is 50 milliseconds.

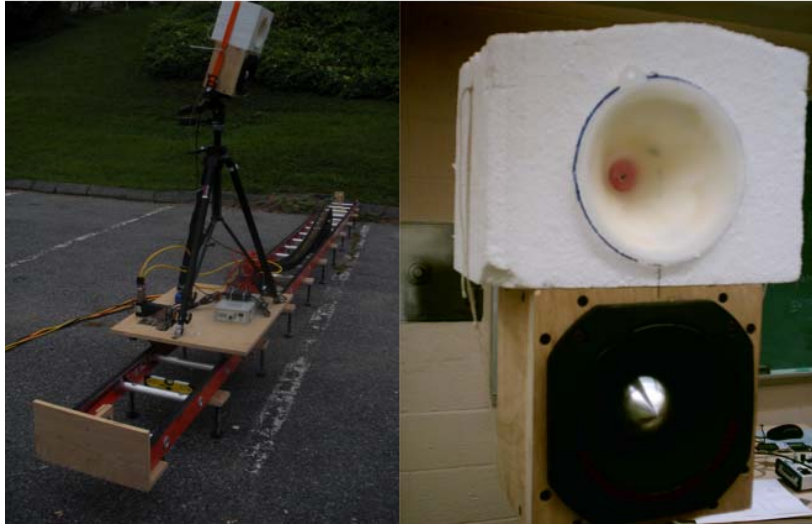


Figure 1 is a photograph of the SAA measurement system mounted on a 6.3 m rail. The transceiver is mounted on a tripod that is supported by a motorized platform that traverses the rail. The inset is a close up view of the acoustic transceiver.







Figure 2 The photograph on the left shows an operator initiating a data collection from the mobile rack. The photograph on the right shows a typical experimental configuration where a number of targets are arranged within the measurement field of the SAA system.

3. TARGET DESCRIPTIONS

A variety of targets were insonified, including: foam blocks [#1 - #3], a bowling ball, a plastic ball, a metal ball, concrete blocks, MON-50, claymore (non-US) landmine, a foam cover panel, acoustic tiles, rocks, and loose branches

with and without leaves. We report here on a subset including: foam blocks, a concrete block, a bowling ball and smaller diameter plastic and metal spheres. Table 2 below provides a brief description of each target.

Table 2 contains a brief description and photographic of each target.

Target	Dimensions, cm L x H x D or Dia.	Weight, Kg	Description	Graphic
Block #1	40.0 x 19.7 x 2.2	1.53	Styrofoam block with brown grout coating.	
Block #2	40.0 x 19.7 x 22.2	8.62	Weighted foam block with grey grout coating.	
Block #3	41 x 21 x 21	4.10	Foam block with grey grout coating.	
Block #4	39.4 x 14.3 x 14.3	11.11	Concrete masonry unit (typical block)	
Bowling ball	22.2	7.03	Typical bowling ball	see Figure 3
Metal sphere	7.3	1.19	Chrome plated metal	see Figure 3
Plastic sphere	7.0	0.14	Solid plastic, black in color	see Figure 3

Ground surface targets were placed flush on weathered asphalt. The transceiver was directed to the targets and oriented with a depression angle of 17.5°. Each of the spheres positions was fixed across the data collections, however the three blocks were interchanged for the below reporting. Coordinates for each target is indicated below in Table 3.

Table 3 Ground coordinates of the targets relative to the center of the rail.

Target	Coordinates, m
Blocks #1 - #4	(0, 2.84)
Plastic Sphere	(-0.69, 4.47)
Bowling Ball	(0, 5.50)
Metal Sphere	(0.69, 4.47)



Figure 3 illustrates the typical target layout as viewed from the transceiver at ground coordinates (0,0).

4. IMAGE PROCESSING AND TARGET FEATURE CHARACTERISTICS

4.1 Wavefront Reconstruction and Motion Compensation

The imaging algorithm that is used to process the SAA data is a Fourier-based approach that is known as *wavefront reconstruction*⁽²⁴⁾. The algorithm was originally developed for processing Synthetic Aperture Radar (SAR) data. SAR wavefront reconstruction algorithm is based on the assumption that the radar-carrying platform stops, makes a measurement, and then moves to its next coordinates on the synthesized aperture (stop-and-go approximation). This is a very good approximation for radar waves that travel at the speed of light, while the platform speed is around 100 m/sec.

In the case of airborne SAA, where the wave propagation speed is around 340 m/sec, this approximation is not valid. In fact, we have developed a modified version of the SAR wavefront reconstruction for the SAA data that does not use the stop-and-go approximation⁽²⁵⁾. For the ground-based SAA data of our experiment, the platform speed is sufficiently small so that both the SAR and SAA wavefront imaging algorithms yield almost identical results.

The current SAA data collection system is not equipped with an INS (GPS and IMU) system. However, it has a wheel-encoder that provides information on the platform speed along the motion path; the wheel-encoder does not provide any data on any unknown motion of the platform on the plane that is perpendicular to the motion path, e.g., wobbling of the transmitter/receiver. We used the wheel-encoder data to perform motion compensation along the motion path.

Figures 4-7 show the reconstructions for the four setups. Note that the SAA images of the four blocks look quite similar; they all appear to be flat and flashing structures in the scene. Furthermore, the SAA images of the bowling ball, metallic ball and plastic ball all appear as *blobs*. Thus, there are no distinct features in the SAA images of the blocks and the balls that could be exploited for conventional pattern-based ATR algorithms. The question then becomes whether an alternative SAA information base exists for ATR for the SAA system.

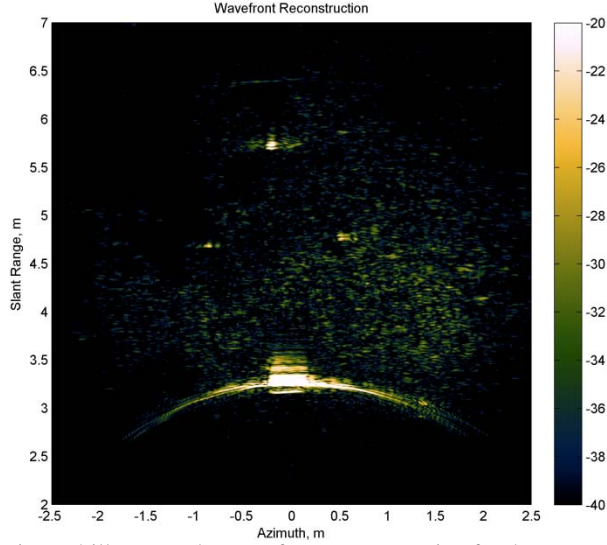


Figure 4 illustrates the wavefront reconstruction for the set-up to include block #1.

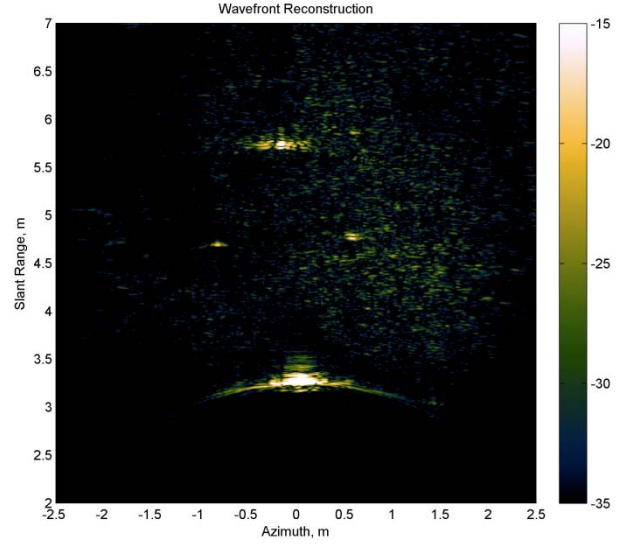


Figure 5 illustrates the reconstruction to include block #2.

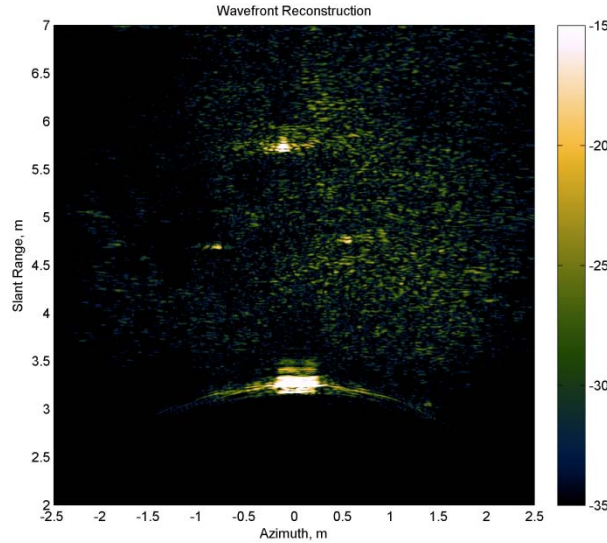


Figure 6 is the reconstruction that includes block #3.

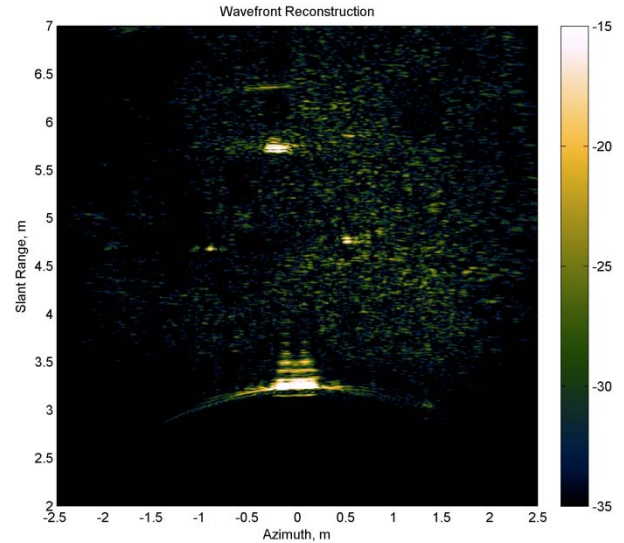


Figure 7 is the reconstruction that includes block #4.

4.2 Signature Extraction via Digital Spotlight Inverse Imaging

The SAA signature of these targets in the original measurement domain, that is, the acoustic frequency and aspect angle domain, reveal more distinct features for ATR purposes. Why didn't we use these data in the first place? (Why do we have to perform imaging?) The answer is that the measured data are a mixture (sum of) the signatures of all targets in the imaging scene and, thus, cannot be separated without further processing (imaging). We have developed a method to reconstruct the SAA/SAR signature of a target from its formed SAA/SAR image⁽²⁴⁾.

In an SAA image, each target appears localized (focused) around a region; this is not the case in the original measurement domain with the *hyperbolic* SAA signatures⁽²⁴⁾. We can extract each "suspected" target image; this process is called *digital spotlighting*. Then, we perform the inverse of the signal-processing algorithm that converted the original measured data into the SAA image to reconstruct the hyperbolic SAA signature of the suspected target; this process is called *inverse imaging*.

Constructing reliable and robust information that are least-affected by the *system errors* has also led us to use digital-spotlight inverse imaging for ATR purposes. Wavefront reconstruction provides high fidelity imagery using the platform wheel-encoder motion information (via motion compensation). As mentioned earlier, due to unknown

vibrations (wobbling) of the platform, accurate motion information is not available on the plane that is perpendicular to the motion path; this causes blurring in a target image signature. Unknown components (such as vibration motion errors in SAA) in a detection or estimation system that carry no useful information, but adversely affect results, are called *nuisance parameters*; an optimal detector/estimator is unaffected by nuisance parameters.

Blurred signature of a target in an SAA image is not an optimal input for ATR since it is altered by vibration motion errors (nuisance parameters). Meanwhile, a target magnitude SAA signature in the original measurement domain can be shown to be approximately unaffected by vibration motion errors. (The vibration motion errors predominately corrupt the phase information.) Moreover, it can be shown that the magnitude signature is also a more reliable database for ATR purposes when a target is *obscured*. The target magnitude information versus acoustic frequency and aspect angle is the output of the digital-spotlight inverse imaging algorithm.

These signatures for the bowling ball and metal and plastic spheres are shown in Figures 8-10. Note that the bowling ball exhibits a wide-beamwidth and wide-bandwidth signature within the operating band of the transceiver ([5,15] kHz band and beam angle of plus/minus 15 degrees). Meanwhile, the smaller metal and plastic balls show more energy at the upper band of [8,15] kHz where the wavelengths are smaller (as anticipated). Moreover, their beam pattern is different from that of the bowling ball. Figure 11 shows the spectra of these balls at the broadside. Note that the three balls exhibit different spectral signatures (peaks and nulls).

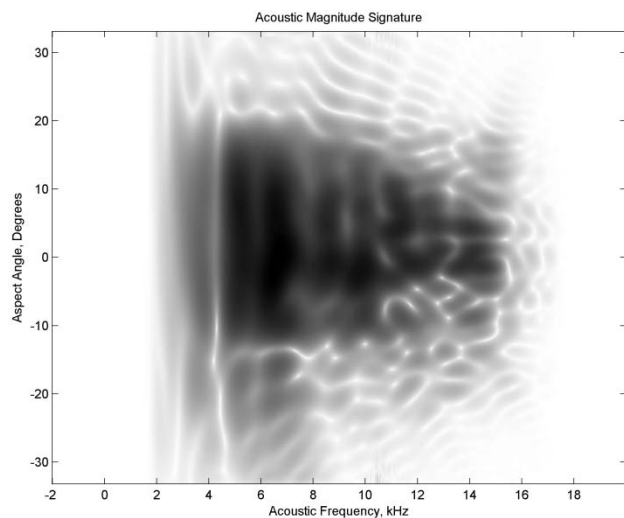


Figure 8 shows the acoustic magnitude signature for the bowling ball.

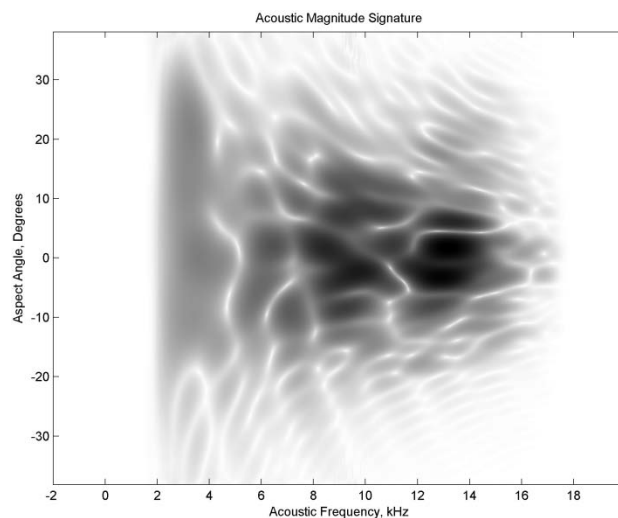


Figure 9 is the acoustic magnitude signature for the metallic sphere.

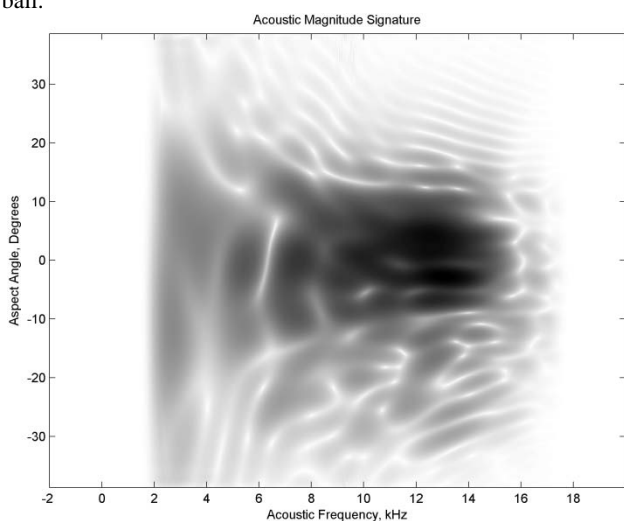


Figure 10 is the signature of the plastic sphere.

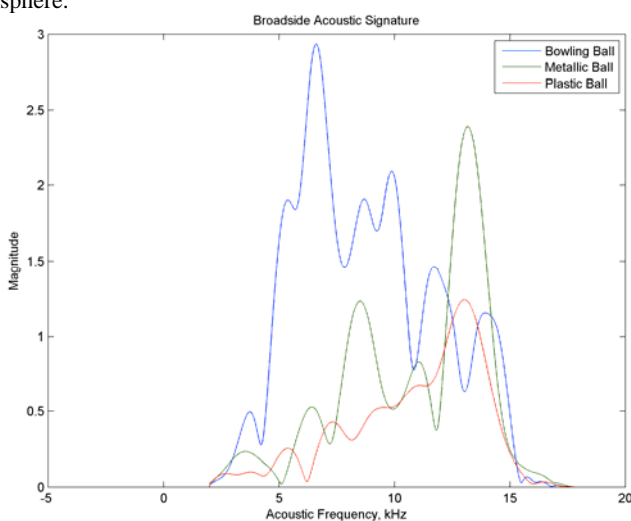


Figure 11 broadside spectra for each of the spherical targets.

Similar results are shown for the four blocks in Figures 12-15. All blocks exhibit narrower signatures in the aspect angle domain (beamwidth) as compared to the balls. Figure 16 shows the spectra of the four blocks at the broadside. Note that the blocks exhibit different spectral signatures (peaks and nulls).

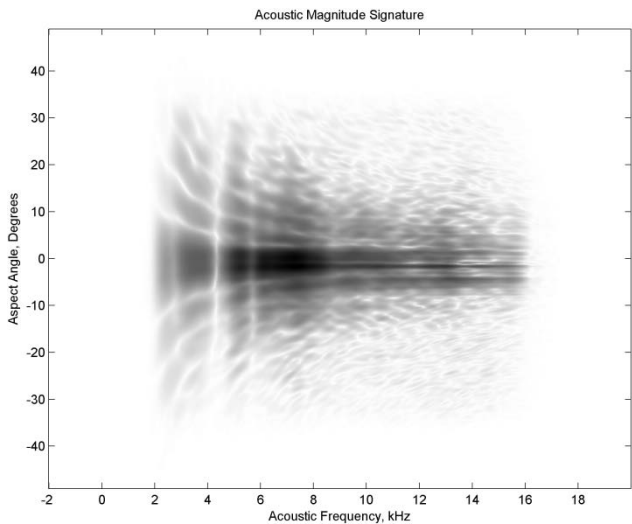


Figure 12 is the signature of block #1.

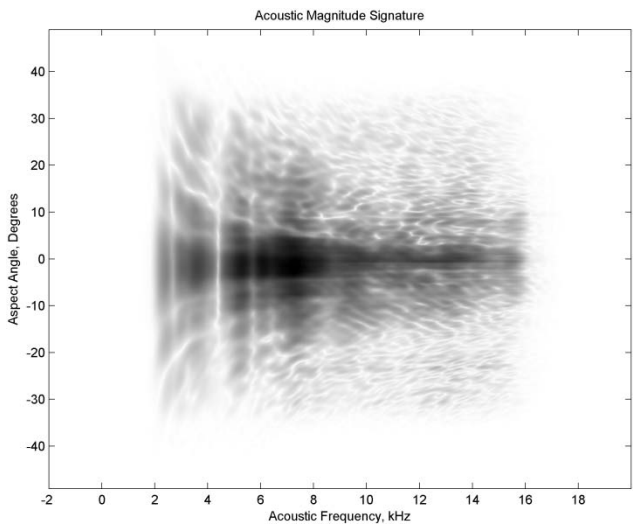


Figure 13 is the signature of block #2.

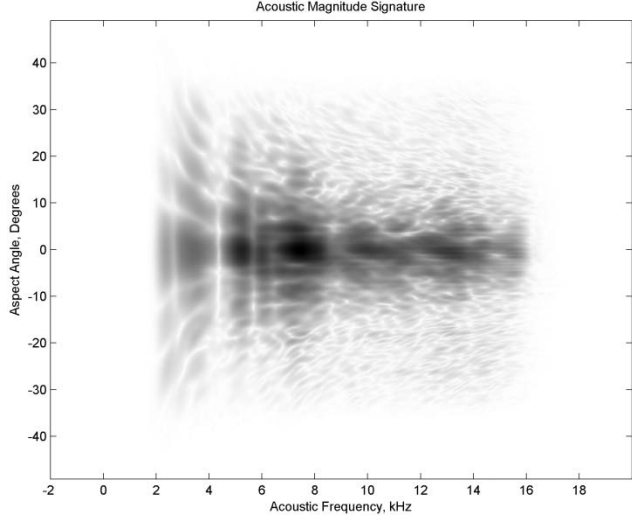


Figure 14 is the signature of block #3.

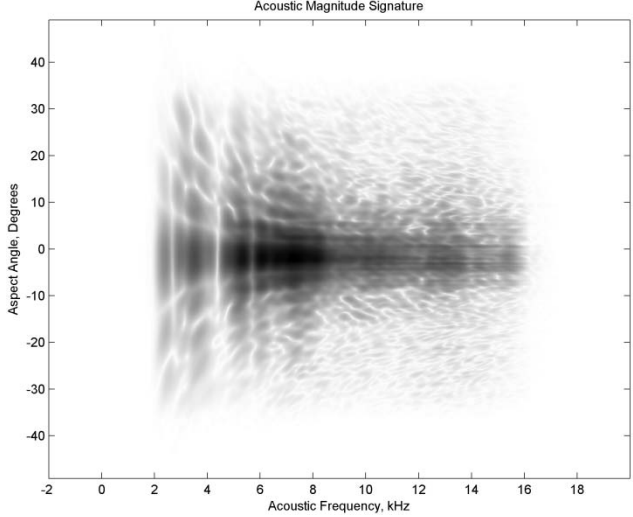


Figure 15 is the signature of block #4.

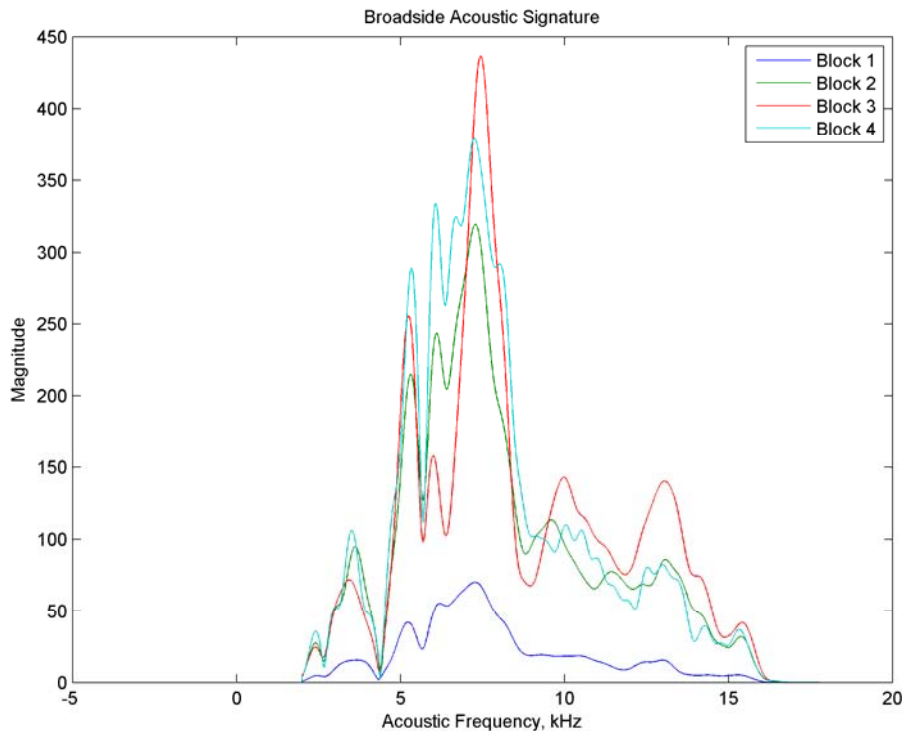


Figure 16 illustrates the broadside-acoustic magnitude for each of the four blocks.

5. SUMMARY

The paper is the second in a series that discusses the progress toward the development of a SAA system. The transceiver is mounted on a portable rail. By moving along the rail, the transceiver can continuously collect data allowing the generation of synthetic aperture. Several canonical targets were placed on a weathered asphalt surface and image formation, i.e., wavefront reconstruction, was performed. This allows for the image processing techniques to include target and ground surface scattering analyses. Additionally, a digital spotlighting technique was performed on selected targets to produce aspect angle versus frequency plots. This allows for subsequent spatial and spectral analyses to be performed.

Digitally spotlighted and broadside position preliminary assessment of the selected targets indicate different relative magnitudes and frequency responses. As expected, the spherical targets have lower acoustic cross-section magnitudes and the blocks' flat surface perpendicular to transceiver travel have significantly larger scattering magnitudes. For example, Block #4 is the manufactured concrete block that shows lower broadside-acoustic magnitude compared to the three other grout covered foam blocks.

Further development is necessary to establish calibrated data to better characterize the system, error reduction through improved transceiver position accuracy in all three spatial dimensions, expanded outdoor data collections under varying environmental conditions, and research and development of structural acoustic techniques for scene analysis and target detection and discrimination.

6. ACKNOWLEDGEMENTS

The authors wish to recognize the support from the U.S. Army RDECOM CERDEC Night Vision & Electronic Sensors Directorate and the U.S. Army RDECOM ARL Army Research Office under contract number W911NF-07-R-003-02 and the support from CUA's Mechanical graduate engineering student Mr. Aldo Glean.

REFERENCES

- [1] T. Wang, O. Sjahputera, J. M. Keller *et al.*, "Landmine Detection Using Forward-Looking GPR With Object Tracking." Proc. SPIE 5794, 1080-1088 (2005).
- [2] Y. Sun, And J. Li, "Landmine Detection Using Forward-Looking Ground Penetrating Radar." Proc. SPIE 5794, 1089-1097 (2005).
- [3] K. Stone, J. Keller, K. C. Ho *et al.*, "On The Registration Of FLGPR And IR Data For A Forward-Looking Landmine Detection System And Its Use In Eliminating FLGPR False Alarms." Proc. SPIE 6953, 695314 (2008).
- [4] E. M. Rosen, F. S. Rotondo, And E. Ayers, "Testing And Evaluation Of Forward-Looking GPR Countermining Systems." Proc. SPIE 5794, 901-911 (2005).
- [5] G. Liu, Y. Wang, J. Li *et al.*, "SAR Imaging For A Forward-Looking GPR System." Proc. SPIE 5089, 322-333 (2003).
- [6] R. D. Costley, J. M. Sabatier, And N. Xiang, "Forward-Looking Acoustic Mine Sensing," The Journal Of The Acoustical Society Of America 109(5), 2342-2342 (2001).
- [7] R. D. Costley, J. M. Sabatier, And N. Xiang, "Forward-Looking Acoustic Mine Detection System," Proc. SPIE 4394, 617-626 (2001).
- [8] G. Shippey, And T. Nordkvist, "Phased Array Acoustic Imaging In Ground Co-Ordinates With Extension To Synthetic Aperture Processing," Radar Sonar And Navigation 143(3), 131-139 (1996).
- [9] D. Donskoy, A. Zagrai, And A. Ekimov, "Landmine Vibration Modes," The Journal Of The Acoustical Society Of America 114(4), 2420-2420 (2003).
- [10] N. Xiang, And J. M. Sabatier, "An Experimental Study On Antipersonnel Landmine Detection Using Acoustic-To-Seismic Coupling," The Journal Of The Acoustical Society Of America 113(3), 1333-1341 (2003).
- [11] C. A. Dimarzio, T. Shi, F. J. Blonigen *et al.*, "Laser-Induced Acoustic Landmine Detection," The Journal Of The Acoustical Society Of America 115(5), 2383-2383 (2004).
- [12] D. Donskoy, "Nonlinear Seismo-Acoustic Landmine Detection," The Journal Of The Acoustical Society Of America 115(5), 2382-2382 (2004).
- [13] J. S. Martin, W. R. Scott, Jr., P. H. Rogers *et al.*, "Ultrasonic Displacement Sensor For Seismic Land Mines Detection," Proc. SPIE 4742, 606 (2002).
- [14] J. M. Sabatier, And V. Aranchuk, "An Acoustic Landmine Detection Confirmatory Sensor Using Continuously Scanning Multibeam Ldv," The Journal Of The Acoustical Society Of America 115(5), 2416-2416 (2004).
- [15] J. M. Sabatier, R. D. Burgett, And V. Aranchuk, "High Frequency A/S Coupling For Ap Buried Landmine Detection Using Laser Doppler Vibrometers," Proc. SPIE 5415(1), 35-41 (2004).
- [16] Bishop, S., [Investigation Of Mechanical Excitation As A Means For Buried Landmine Detection], The Catholic University Of America, Washington, 7-10 (2008).
- [17] Raichel, D. R., [The Science And Applications Of Acoustics], Springer-Verlag, New York, 233-235 (2000).
- [18] P. Venugopalan, P. D. Deshpande, M. A. Chitre *et al.*, "Broadband Acoustic Reflectivity And Its Application To The Characterisation Of Materials," Oceans '04. Mts/IEEE Technoo-Ocean '04, 4(4), 2055-2059 (2004).
- [19] M. W. Muller, J. S. I. Allen, W. W. L. Au *et al.*, "Time-Frequency Analysis And Modeling Of The Backscatter Of Categorized Dolphin Echolocation Clicks For Target Discrimination," The Journal Of The Acoustical Society Of America 124(1), 657-666 (2008).
- [20] Y. Nakamura, I. Yamaguchi, T. Tanaka *et al.*, "Buried Object Detection With Synthetic Aperture Sonar," International Symposium On Underwater Technology, 27-31 (2004).
- [21] F. L. Scarpa, F. Dallochio, And M. Ruzzene, "Identification Of Acoustic Properties Of Auxetic Foams." Proc. SPIE 5052, 468-474 (2003).
- [22] H. Uberall, "History Of Resonance Scattering Theory In Acoustics And Its Applications To Target Recognition." Proc. SPIE 1960, 350-361 (1993).
- [23] S. Bishop, T. Woods, J. Vignola *et al.*, "Synthetic Aperture Acoustic Measurements Of Stationary Suspended Cinderblock And Surrogate Substitutes." Proc. SPIE 7303, 73030j-11 (2009).
- [24] M. Soumekh, [Synthetic Aperture Radar Signal Processing], Wiley, New York, 24 (1999).
- [25] M. Soumekh, "Airborne Synthetic Aperture Acoustic Imaging," IEEE Trans. Image Processing 6(11), 1545-1554 (1997).